Available online at www.sciencedirect.com
SCIENCE DIRECT®
Carbohydrate Research 339 (2004) 975–983
Carbohydrate RESEARCH

The heparin–Ca^{2+} interaction: the influence of the O-sulfation pattern on binding

Franck Chevalier, Ricardo Lucas, Jesús Angulo, Manuel Martin-Lomas and Pedro M. Nieto*

Grupo de Carbohidratos, Instituto de Investigaciones Químicas, CSIC, Américo Vespucio s/n, Isla de la Cartuja, 41092 Seville, Spain

Received 17 October 2003; accepted 12 December 2003

Abstract—The specific binding of Ca^{2+} to synthetic hexasaccharide models of modified heparin has been investigated by NMR and molecular modeling and compared with previous results on a model of regular heparin. These two models represent the regular region of heparin lacking one type of O-sulfate group, either at C-6 of glucosamine or at C-2 of iduronate. The NMR experiments show different responses to the presence of Ca^{2+}. In the case of the compound lacking O-sulfate groups at C-2, the results are indicative of specific binding similar to that observed for the regular heparin, while the model lacking sulfate groups in position 6 interacts more weakly with Ca^{2+}. In order to understand the basis of this difference, a molecular modeling study based on a rigid body docking approach of the interaction of these carbohydrates with Ca^{2+} and Na^{+} was performed. We have found that the results are strongly dependent on the starting orientation of the lateral side chains of the charged groups of the carbohydrate, and that the best agreement with the experimental results is obtained when the starting conformations are taken from previous simulations in the presence of Ca^{2+}.

Keywords: Heparin; Calcium interaction; Molecular modeling; NMR spectroscopy

1. Introduction

Heparin is a negatively charged glycosaminoglycan constituted mainly by a basic repeating disaccharidic unit made of α-(1→4) linked L-iduronic acid and D-glucosamine units.[1,2] This basic unit is found variously sulfated and its sulfation pattern is the main source of the structural polydispersity of heparin. Although other arrangements are also possible, heparin is typically sulfated at positions 6 and 2 of glucosamine and 2 of iduronate. The same substitution pattern is frequently found in heparan sulfate but, in this case, is not the major component of the polysaccharide.[1,2] Heparin and heparan sulfate interact with extracellular proteins regulating their activities,[1–4] and in several cases these interactions involve cations such as Ca^{2+} or Mg^{2+}.[5,6] Although the mechanisms by which the cation modulates heparin activity are often unknown, it is accepted that cations can interact with heparin in different manners. These polysaccharides, due to their high linear charge, behave as polyelectrolytes displaying specific physicochemical properties.[7] The polyelectrolytes can bind counterions either territorially or site-specifically by means of long-range electrostatic forces or by specific short-range interactions, respectively. In the territorial binding, the hydrated counterions are delocalised in a volume around the polyion while in the site-specific mode, complexes with defined structure are formed.[7] It has been concluded that while the binding of Ca^{2+} or Zn^{2+} to heparin is primarily site specific, this is not in the case of other physiological metal ions as Na^{+} or Mg^{2+}, which are always territorially bound.[8] Also it has been found that the carboxylate groups of the iduronate residues are essential for Ca^{2+} specific binding as this capability is lost when heparin is chemically modified as methyl ester or when these groups are protonated.[8] A

* Corresponding author. Tel.: +34-95-448-95-65; fax: +34-95-446-05-65; e-mail: pedro.nieto@iiq.csic.es

0008-6215/$ - see front matter © 2004 Elsevier Ltd. All rights reserved.
doi:10.1016/j.carres.2003.12.023

similar role has been attributed to the sulfamido group of the glucosamine residues as heparin fragments lacking of this function are unable to bind Ca^{2+} as the regular heparin.[9,10] However, there are evidences that the binding properties are not affected by the loss of the 2-*O*-sulfate groups of the iduronate residues.[10,11] These results taken together strongly suggest the existence of a Ca^{2+} binding site in the structure of heparin.

Because of its physiological importance, we have investigated the interaction of Ca^{2+} with heparin using synthetic models, which provide homogeneous and well defined structures, as well as simpler NMR spectra.[12,13] We have previously studied two synthetic models of the regular region of heparin: the basic disaccharide unit and hexasaccharide **1**[14] observing ^1H NMR changes consistent with Ca^{2+} specific binding.[12] The existence of metal binding sites in heparin was also explored by molecular dynamics simulations of **1** in the presence of Ca^{2+}, which suggested that some regions of heparin were especially favourable for the interaction with Ca^{2+}.[12] In order to quantify this interaction, we made use of a computational protocol based on rigid body docking, which was able to reproduce the binding selectivity favourable to Ca^{2+} as opposite to Na^+ or Mg^{2+}.[13]

Now, we have extended our NMR studies on Ca^{2+}–heparin interaction to two more synthetic hexasaccharides (**2** and **3**),[15] which lack the sulfate groups in position 2 of the iduronate and 6 of the glucosamines, respectively. These results, combined with those for **1**, should contribute to estimate the relative importance of heparin O-sulfation pattern in the specific interaction with Ca^{2+}. We also have explored the suitability of the computational procedure used for the quantitative analysis of the potential interaction sites of **1** to other substitution patterns as those present in **2** and **3**.

2. Results

2.1. NMR

We have recorded 1D and 2D NMR spectra of the model hexasaccharides **2** and **3** in the presence of different concentrations of calcium chloride in order to verify if calcium interacts specifically with them (Fig. 1). The chemical shift displacement of the signals was followed by analysing the 1D spectra using standard 2D NMR techniques when necessary. We have focused the analysis on the resonances of H-1 and H-5 of the iduronate residues as they display the largest variations and appear in both hexasaccharides in a nonoverlapped region of the spectra. The chemical shift values for H-1, H-2 and H-5 resonances and their variation in the presence of Ca^{2+} are shown in Tables 1 and 2.

The chemical shifts of **1**, **2** and **3** in absence of Ca^{2+} are very similar (Table 1), and the observed differences can be interpreted in terms of the effect of the electronegativity of the heteroatoms of the sulfate groups. Such variations of the chemical shift depending on the O-substitution are well known for this type of compounds from the studies on heparin and heparin sulfate

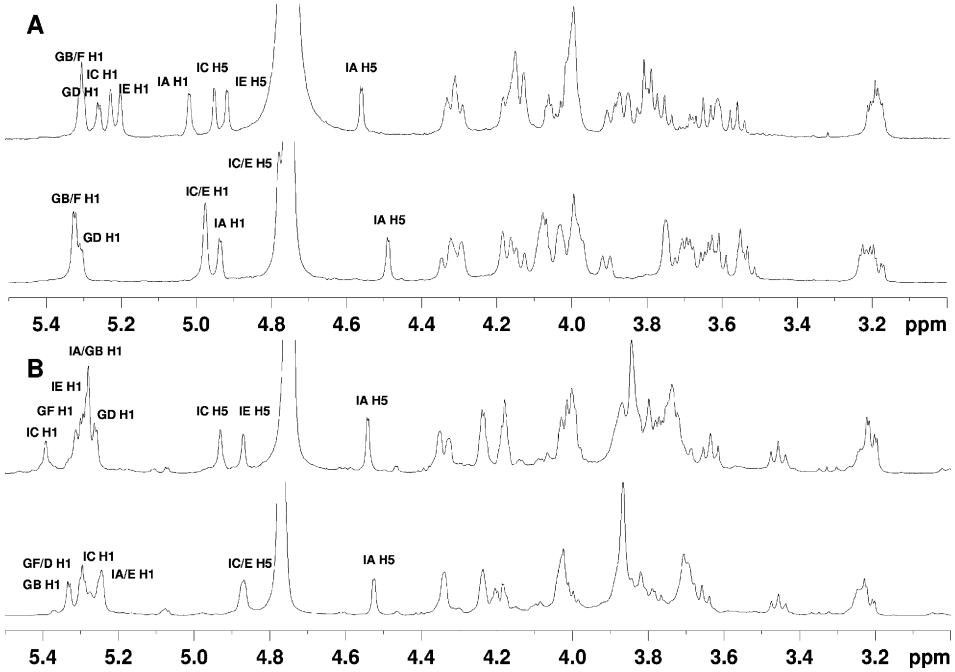

Figure 1. ^1H NMR spectra (D_2O, 298 K, pH* = 7.2, 500 MHz) of (A) **2**, and (B) **3**; sodium salt (bottom), in the presence of 4.5 mol equiv of calcium chloride (top).

Table 1. Chemical shift of selected signals for the sodium salts of **1**, **2** and **3** at 298 K, 500 MHz in D_2O

	Ido A			Ido C			Ido E		
	H-1	H-2	H-5	H-1	H-2	H-5	H-1	H-2	H-5
1	5.22	4.16	4.51	5.25	4.32	4.82	5.20	4.31	4.80
2	4.94	3.56	4.49	4.98	3.77	4.80	4.98	3.76	4.79
3	5.23	4.16	4.51	5.25	4.32	4.85	5.24	4.31	4.84

Table 2. ^1H Chemical shift variation for selected protons for hexasaccharides **1**, **2** and **3** in the presence of 6, 4.5 and 4.5 mol equiv of Ca^{2+}, respectively, with respect to the Na^+ salt[12]

	Ido A			Ido C			Ido E		
	H-1	H-2	H-5	H-1	H-2	H-5	H-1	H-2	H-5
1	0.08	0.04	0.05	0.17	0.06	0.11	0.11	0.04	0.05
2	0.07	0.06	0.07	0.24	0.11	0.15	0.22	0.10	0.12
3	0.04	−0.03	0.02	0.09	0.00	0.06	0.06	−0.03	0.02

derivatives,[16,17] and in this sense the synthetic compounds behave as the natural derivatives.[18]

The binding of calcium to the hexasaccharides was followed by titration with calcium chloride (Table 2 and Figs. 2 and 3). The specific interaction could be detected by the nonlinear behaviour of the increment of the chemical shifts as opposite of the linear response, expected in case of nonspecific binding.[12] While in the case of **2,** an appreciable variation on the chemical shift of the signals upon calcium chloride addition was observed, a smaller effect was detected for **3** (Fig. 1). The changes on the chemical shift of significant signals of **3** were smaller than 0.05 ppm except for the central iduronate anomeric proton (0.10 ppm), and in all cases the variations were significantly smaller than those found for **1** and **2**. The profile of the chemical shift increment with Ca^{2+} concentration shown in Figure 3 shows a complex behaviour with several inflexion points, which indicates clearly some type of specific binding. This type of response is comparable with the observed for **1**[12] (Fig. 3), which reproduces the regular region of heparin, and has shown a specific interaction with calcium. The effect of the addition of Ca^{2+}, within the same residue, is larger for the iduronate anomeric protons than for H-5 protons and it is smaller for the H-2 ones (Fig. 2). This trend as well as the downfield shift of these signals correspond with the findings for the regular compound **1**.[12] There is also a clear influence of the position of the residue along the chain on the magnitude of the chemical shift variation. The inner iduronate protons display

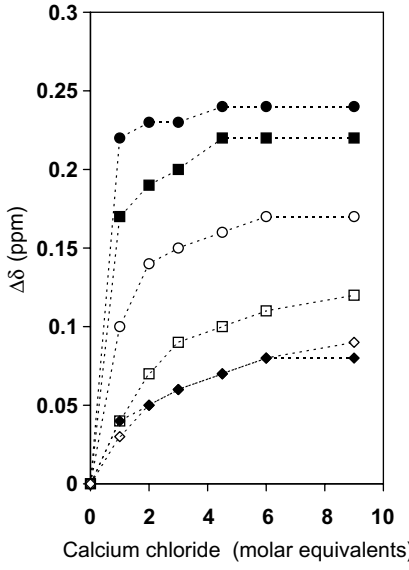

Figure 2. Variation of chemical shift values of proton H-1 (dots), H-2 (lines) and H-5 (broken lines) of iduronate residues at position 1 (diamonds), 3 (circles), and 5 (squares) of **2** with the concentration of calcium chloride.

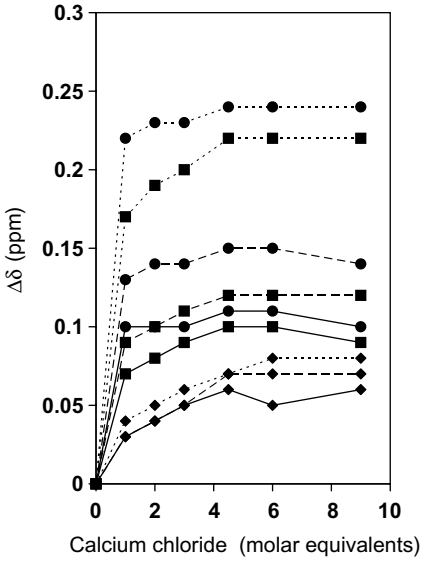

Figure 3. Variation of chemical shift values of the anomeric protons of iduronate residues at positions 1 (diamonds), 3 (circles), and 5 (squares) of **1** (filled) and **2** (open) with the concentration of calcium chloride.

larger increments than the equivalent protons from other residues while those from the terminal ones are the less affected by the cation. Such observation also agrees with the behaviour of the regular model **1**.[12] The anomeric protons of the glucosamines for both compounds are also affected but they suffer a small upfield shift lower than 0.05 ppm in all cases.

We noticed that once the added cation neutralises the hexasaccharide **2** negative charges, further addition of calcium chloride does not modify the chemical shifts; this is not the case for **1** where some signals still show a small drift after this point. This saturation behaviour is observed as a plateau in the titration curve approximately at 6 and 4.5 equiv of calcium chloride for **1** and **2**, respectively. As **1** and **2** feature 12 and 9 negative charges, respectively, at pH 7 these equivalence points represent the oligosaccharide charge compensation by the added Ca^{2+}. This behaviour is indicative that the Ca^{2+} interaction with heparin is as stronger as to displace all the Na^+ from the oligosaccharides.

The interaction of these oligosaccharides with Ca^{2+} does not affect their overall conformation. The global structure of heparin like molecules adopts a helix shape,[19] giving rise to an elongated molecule generated by the overall structure of the saccharidic ring backbone. This basic structure is driven by the carbohydrate backbone and is rather independent of the particular sulfation pattern considered.[4,18] We have previously demonstrated by NMR that the presence of Ca^{2+} does not alter appreciably the shape of **1** as to be detected by the analysis of interresidue key NOE peaks, which must be affected if such structure is changed.[12] The interglycosidic NOE patterns of **2** are essentially the same in presence of Na^+ or Ca^{2+} and, in both cases, equivalent to that of **1**.

Other structural feature of this type of compound easily detected by NMR is a characteristic conformational equilibrium of their iduronate rings, which comprises two conformations: the $^1C_4$ chair and ^2S_O skew boat (Fig. 4).[19,20] Interestingly, this equilibrium does not break the helical symmetry of these compounds, although it may change the orientation of some exocyclic groups generating local changes in the spatial arrangement of the sulfate groups.[18] This equilibrium is easily detected by the observation of the NOE between

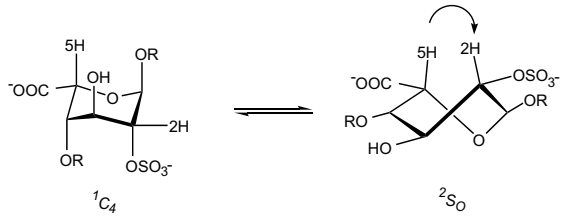

Figure 4. Iduronate conformational equilibrium between conformers $^1C_4$ and ^2S_O showing the H-2–H-5 exclusive NOE.

H-2 and H-5 protons together with averaged intraannular coupling constants accounting for both conformations.[2] While the NOE is exclusive of the ^2S_O conformation and is symptomatic of its presence in the equilibrium, the analysis of the intraannular coupling constants can be used to quantify the conformer populations.[2] We have previously observed an influence of the presence of Ca^{2+} in the iduronate conformational equilibrium as the complexation of the cation causes an enhancement of the $^1C_4$ population for **1** (from 55% to 70%) as well as in a model disaccharide.[12,13] Unfortunately a similar quantitative analysis was not possible for **2** due to the signal overlapping and line broadening, which prevents the accurate measurement of the coupling constants, nevertheless a partial analysis of resolved signals (data not shown) agrees qualitatively with an increase of the $^1C_4$ population. This observation is also supported by the semiquantitative analysis of the NOE between H-2 and H-5 iduronate protons, which is diagnostic of the ^2S_O conformation.[19] We have observed a decrease of the relative intensity of the H-2–H-5 NOE cross-peaks with increasing concentration of Ca^{2+}, which is indicative of an enhancement of the population of the $^1C_4$ conformation in the equilibrium.

Summarising, we have observed very different responses to the interaction with Ca^{2+} from the two models lacking either 2- or 6-*O*-sulfate groups, with respect to the heparin regular region. While **2**, which is sulfated at the glucosamine 6 position, has a behaviour indicative of specific binding and very close to **1**, the model lacking sulfate groups at this specific position, **3**, shows a less significant response, indicative of a weaker interaction.

2.2. Modeling

In order to explain the differences in the interaction with Ca^{2+} displayed by **1**, **2** and **3** observed by NMR, we decided to evaluate the relative binding energies using the program GRID.[21,22] GRID allows to examine the surface of a target molecule, calculating the interaction energy with the ligand at the molecular surface very efficiently, locating the binding regions. However, it may fail exploring flexible molecules, such as **1**–**3**, as it does not consider properly conformational features because it is based on static structures. We have previously used a combination of molecular dynamics simulations with GRID to study the selectivity of the interaction between **1** and several cations.[13] The procedure used was based on the properties of the MD sampling the conformational space of the carbohydrate side chains and the accuracy of GRID evaluating the interaction. Thus, an ensemble of representative structures was generated from a MD simulation and further analysed by GRID program. This ensemble should represent all the possible structural alternatives as to contain implicitly the

information about the flexibility of the system in order to overcome the limitations of GRID. In our hands, this procedure was able to locate the cation binding site suggested by NMR[12,13] and to reproduce the cation selectivity reported for heparin.[8]

The first stage of the study of **2** and **3** was to optimise the method for the preparation of the ensemble to be used in the evaluation phase. We initially assumed that the geometry of the binding site should be very similar to the one previously found in **1**, and the values of the angles Φ, Ψ, ω and χ (see Fig. 5) should be similar as well. This assumption was based on NMR and MD studies of the sodium salts of **1**, **2** and **3** that indicated that their general conformational behaviour was essentially the same.[20] Accordingly, we prepared the starting ensemble of **2** and **3** constructing manually the structures using the Φ, Ψ, ω and χ values from the previous study of **1**. All the iduronate residues in these structures were built in the $^1C_4$ chair conformation because the NMR results and previous works[12,13] indicate that this is the most favourable form for the interaction. The results obtained for the interaction of these sets of structures with Ca^{2+} were unsatisfactory because the interaction energies calculated for **2** and **3** were always similar, not reflecting the differences found by NMR indicatives of the specific binding of Ca^{2+} by **2** but not by **3**. We explain this inconsistency by an inadequate choice of the studied ensemble.

In order to take into account possible structural differences between **1**, **2** and **3** in a second approach the initial ensembles of structures were generated from molecular dynamic simulations specifically performed for **2** and **3**.[20,23] In this way, the possible structural differences will be considered. We used previous molecular dynamic simulations of 2 ns in explicit water from a structural study of the free hexasaccharides to generate the ensemble.[18,23] The trajectories were divided in 10 periods of 200 ps, obtaining a representative structure for each one by averaging.[18] The results obtained using this approach were also contradictory with the NMR observations. In order to verify whether this disagreement could be due to the fact that the source MD simulations included Na^+ instead of Ca^{2+}, we created a new set of ensembles for **2** and **3** from MD simulations in the presence of Ca^{2+}. In this case, we did not use explicit water as we were more interested in sampling a region of the conformational space as wider as possible. The results show a different distribution of the torsional angles of some side chains compared with the MD simulations in presence of Na^+. Here it should be noticed that comparable calculations previously performed for **1** did not display such variation. From new MD trajectories we built the corresponding ensembles of structures as combination of the allowed Φ, Ψ, ω and χ angles to be used as input for the analysis made by GRID. A new torsional angle value was considered in the construction of the ensemble if a variation larger than 15° was observed in the corresponding molecular dynamic simulations. The values of torsional angles found using this criterion were different as compared to those previously deduced for **1**, probably as a consequence of the change in the substitution pattern. As in the other ensembles, only the iduronate $^1C_4$ chair conformer was considered in the present study. The accuracy of this choice was confirmed by probing some examples of ^2S_O conformation, which yielded lower interaction energy than the $^1C_4$ chair (data not shown). Finally, this procedure resulted in the construction of four structures for **2** and only one for **3**. The values of the stronger interaction energy found for each model using GRID are shown in Table 3. The higher Ca^{2+} interaction energies of each compound are more favourable for **2** (Table 3, entries 1, 4 and 5) than for **3** while the lower are similar in both cases (Table 3, entries 2, 3 and 5). The magnitude of the larger Ca^{2+} interaction for **2** is similar to that found for **1** and, on the other

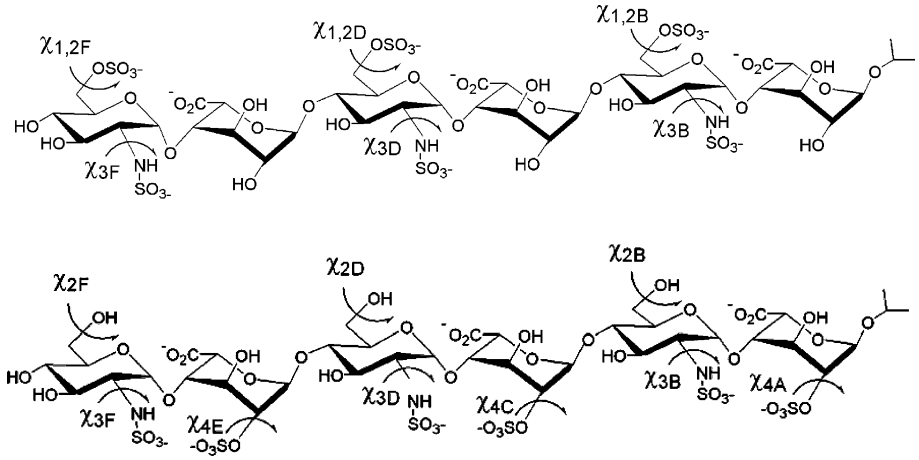

Figure 5. Torsion angles considered for the construction of the ensemble of structures used in the calculation of the cation interaction energy: top, torsion angles considered for **2** and bottom, torsion angles considered for **3**.

Table 3. Interaction energy calculated for **2** (entries 1–4) and **3** (entry 5) conformers

	Energy (kcal/mol)		Torsional angle (°)								
Entry	Ca^{2+}	Na^{+}	χ_{1F}	χ_{2F}	χ_{1D}	χ_{2D}	χ_{1B}	χ_{2B}	χ_{3F}	χ_{3D}	χ_{3B}
1	−90	−47	78	−68	100	−60	−135	66	65	−100	129
2	−78	−44	78	−68	100	−60	−135	66	100	−100	180
3	−77	−43	78	−68	−120	90	120	66	100	−100	180
4	−90	−49	78	−68	−120	90	120	66	65	−100	129
5	−77	−42		−66		−68					

hand, also the Na^{+} interaction energies for **1**, **2** and **3** are comparable.

Concerning the geometry of the binding site, in our previous study of **1** we proposed three different potential sites of interaction of the regular region heparin with Ca^{2+} on the basis of MD simulations and GRID calculations.[13] The first, called A, implied the N-sulfate of glucosamine and the oxygen of the O-glycosidic linkage together with the sulfate in position 2, the carboxylate and the ring oxygen of the preceding iduronate residue; the second one, named B, involved the two glucosamine sulfate groups and the carboxylate of the following iduronate residue; and the last one, C, includes the sulfate groups of both glucosamine and iduronate, but in reverse order as in A. It could be expected that the changes in the sulfation pattern in **1**, **2** and **3** would modify the arrangement of these binding sites. First, the lack of sulfate group at C-6 of the glucosamine in **3** would exclude the existence of B or C type sites, and finally the lost of the iduronate 2-*O*-sulfate groups in **2** would prevent arrangements like A and C. However, the experimental results for **2** and **3** could not be explained using the same binding sites than those for the regular region heparin. Moreover, the exocyclic torsional angles of the calcium salt are dependent on the substitution pattern and the values found for **1** yield inaccurate interaction energies. However, the analysis of the regions of higher interaction of the molecular surface of **2** and **3** allow the location of common favourable sites within the models built for **2**, which are not present in **3**. These sites are similar to the type B ones found in **1**, and involve the carboxylate of the iduronate residue and the N-sulfamide of the previous glucosamine, but now also participates the 6-*O*-sulfate of the following glucosamine residue. Such arrangement is possible for **2** but not for **3**, and therefore it would explain the selectivity found by NMR for the hexasaccharides **1**, **2** and **3** as well as other results on chemically modified heparin that have shown that both carboxylate and N-sulfamide groups are essential for calcium binding.[8–11]

3. Discussion

Heparin and derivatives are anionic polymers that present a wide and complex range of modes of interaction with cations: acting as polyelectrolyte with delocalised binding with some, by forming a specific chelate-like complex with others or even displaying mixed behaviours in some cases. Previous studies have found that Ca^{2+} is specifically bound to heparin, and that glucosamine N-sulfamido and iduronate carboxylate groups are essential for this interaction, while *O*-sulfate groups are less or nonimportant. Interestingly, the selectivity is reversed for Cu^{2+} binding, which is not affected by the depletion of the sulfamido group. There are not many studies about the relative importance of the two more usual *O*-sulfate substituents: those at positions 6 of glucosamine and 2 of iduronate. We have previously studied the interaction of the model hexasaccharide **1**, which contains the structural features of the regular region of heparin with Ca^{2+} by NMR spectroscopy. The results of titration of hexasaccharides **2** and **3** using the same technique indicate that the 6-sulfate group of the glucosamine ring is also essential for the interaction with Ca^{2+} while the 2-iduronate susbtituent seems to be redundant.

Most of the methods and programs used for computational evaluation of molecular interactions have been developed in the fields of protein–protein or protein–drug interaction but it is not always straightforward to use them in small molecule problems, especially when dealing with flexible systems.[24] Such flexibility issues, as the induced fit where the conformation of the receptor changes upon formation of the complex, constitute a challenge for these computational methods. The approaches based on rigid body docking or on surface analysis are usually very fast but they do not consider intrinsically the flexibility of the interacting molecules. This shortcoming can be overcome by including procedures for the generation of new local structures during the process of analysis of the interaction.[13] Other approaches, more suitable to deal with problems with high degree of flexibility, are often based on simulated annealing by molecular dynamics simulation. Also based on molecular dynamics simulations there are methods that allow the accurate evaluation of the interaction energy by analyzing the MD trajectories of the solvated partners and the complex.[25] Unfortunately, these approaches are very demanding on computational time. We have developed a protocol based on the calculation of the interaction energy using a rigid body method, as implemented in GRID, which accounts for the flexibility of the carbohydrate by considering an

ensemble of structures, which should represent adequately the accessible conformational space. In that protocol, the ensemble is generated rapidly from MD simulations, generally performed in vacuo as the purpose is the generation of a wide family of structures. This ensemble is then evaluated for the interaction with cations employing GRID. Concerning the interaction with cations this method is only considering the influence of the electrostatic landscape of the host molecule as it only considers electrostatic and Lennard-Jones potentials and therefore no quantum mechanics effects are considered. However, in our hands this protocol has been able to predict the binding sites of the regular region of heparin in **1** and even to reproduce its selectivity towards Ca^{2+} versus Na^{+} or Mg^{2+}.[13] In this way the method represents a very fast tool for a first survey of the molecular electrostatic landscape, locating potential cation binding regions by affording a quick general analysis of the interaction in spite of its background theoretical limitations.

In order to assess the applicability of the method we have applied it to the interaction of **2** and **3** with Ca^{2+}. If previously this approach was able to reproduce the selectivity of **1** towards different cations, now we have tested if it is able to model how differences on the carbohydrate change their binding properties. Contrary to the previous performance we found persistent problems simulating the difference in binding properties of **2** and **3** that were finally overcome by changing the method used for the creation of the ensemble used for the final GRID calculation. This fact is reflecting the problems associated to the inherent flexibility of this system where small changes on the torsional angles of the sulfate groups cause very large variations on the electrostatic landscape. Additionally to this observation it can be also argued that the variations on exocyclic groups have a larger influence in the overall shape in these small oligosaccharides than in larger molecules as proteins. From this work, it can be deduced that this approach is not still as mature as to be used independently of some additional experimental knowledge. However, if combined with experimental data, it could be a valuable tool for a fast analysis of the glycosaminoglycan–cation interaction.

A preliminary analysis of the experimental results together with the previous modeling results for **1** could be interpreted if Ca^{2+} was bound by an A type site, present in **1** and unviable in **3** but possible in **2** considering as binding group the oxygen atom of the iduronate 2-hydroxy group instead of the 2-sulfate group. However, this previous hypothesis was not confirmed by the computational evaluation, which suggests essential differences between the GRID potential binding regions found for **2** with the binding sites proposed for **1**. The new sites observed for **2** are similar to the B sites proposed for **1** but complemented with additional interactions from the glucosamine 6-sulfate (Fig. 6). The higher

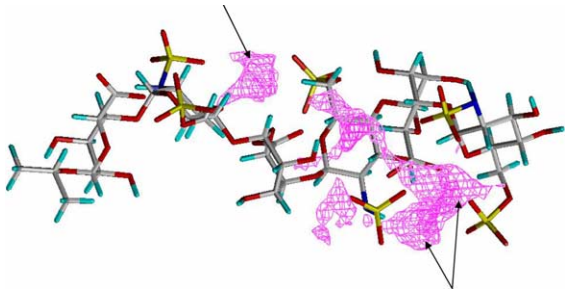

Figure 6. Structure of hexasaccharide **2** and volumes of the regions of the interaction for Ca^{2+} within 15 kcal/mol above the lowest values. The arrows indicate the B-like interaction sites.

interaction energy volumes are distributed asymmetrically along the oligosaccharide structure being more profuse at the middle and at nonreducing end than at the reduced end. This observation is in agreement with the observed chemical shift changes, which are smaller for the first iduronate ring increasing for the residues at positions 3 and 5. These regions of higher binding energy are close to the carboxylate groups, which could explain the large chemical shift variation of iduronate H-5 protons due to inductive effect from the neighbour carboxylate. The resolution of the complex with the cation obtained from this calculations is lower than a molecular mechanics optimisation and therefore we cannot give a more detailed picture of its local geometry. However, as the fingerprint of the chemical shift changes is similar to that observed for **1,** it can be proposed an analogue set of interactions with the metallic ion involving the anomeric and endocyclic oxygens of the iduronate residues, being this possibility not in contradiction with the space distribution of the interaction regions calculated for **2**.

These results taken together with previous studies,[8–11] seem to indicate that the carboxylate group of iduronate together with the N-sulfamido and the 6-*O*-sulfate of glucosamine are essential for the interaction of heparin and derivatives with Ca^{2+}, while the sulfate group at position 2 of the iduronate ring is not. The analysis by molecular modeling of the binding of Ca^{2+} to **1**, **2** and **3**, suggest several alternative modes of interaction depending on the local arrangement of the exocyclic groups. Such suggestion would explain results from other studies in which it was observed that Ca^{2+} binding can accommodate a broad range of spatial distribution of the anionic groups.[10]

4. Experimental

4.1. NMR

All hexasaccharides were prepared as described previously and carefully purified by column chromatography.[14,15] All samples were eluted through Sephadex G-25

first with water (5% NaCl) and then lyophilised with 1:9 EtOH–water. The samples were subjected to a final elution on Dowex cationic exchange resin followed by neutralisation with NaOH until neutrality. Before preparing of the NMR samples, all compounds were deuterium interchanged by at least three cycles of 'freeze-drying' followed by dissolution in deuterated water. For **2**, a 5.48 mM sample in D_2O has been used and the pH* was adjusted to 7.22. For **3**, a 5.71 mM sample in D_2O has been used and titrated with the same calcium chloride solution; the pH* was adjusted to 7.2–7.6. Titration was performed by adding quantities of a 0.56 M calcium chloride solution in D_2O 99.99%.

NMR experiments were recorded on a Bruker AVANCE 500 spectrometer at 298 K. DQF-COSY,[26] TOCSY[27] and NOESY[28] experiments were recorded using manufactures pulse sequence programs enhanced with *z*-axis pulsed field gradients when possible. All experiments were recorded in the phase sensitive mode using the TPPI (time proportional phase increment) method.[29] NOESY experiments were acquired with a mixing time of 400 ms, 512 increments of 24 experiments and 2048 complex points. TOCSY experiments were acquired with 512 increments of 24 experiments and 2048 complex points and a mixing time of 60 ms. DQF-COSY experiments were acquired with 512 increments of 24 experiments and 2048 complex points. Processing and analysis were performed using XWINNMR, zero filling was used in all cases, at least twice, and all fids were multiplied by a shifted squared sine function previously to be Fourier transformed.

4.2. Modeling

Molecular Dynamics in vacuo have been run with AMBER6 force field,[30] including additional parameters for carbohydrates provided by Glycam93.[31] Ten nanosecond run with a timestep of picosecond were recorded for hexasaccharides **2** and **3** including nine Ca^{2+} cations as counter ions. The electrostatic energy term includes a dielectric constant proportional to the distance ($\varepsilon = 5r$), with a simulated temperature of 298 K. Weighting of the relative hydrogen-bonding energy terms have been varied by gradual and continuous increase of it. The charges used were obtained from PIM parameters.[32] The dihedral angles ϕ, ψ and ω are defined as O-5–C-1–O-1–$C_{x'}$, C-1–O-1–$C_{x'}$–$C_{x+1'}$, where $C_{x'}$ and $C_{x+1'}$ are the aglyconic atoms, and O-5–C-5–C-6–O-6, respectively, following IUPAC definition. Sulfate groups orientations were defined as C-5–C-6–O-6–S-6 (named $\chi 1$) and OR–C-5–C-6–S-6 (named $\chi 2$) for groups in position 6 of glucosamine residues in **2**, C-1–C-2–N-2–S-2 for glucosamine in **3** (named $\chi 3$) and C-1–C-2–O-2–S-2 for (named $\chi 4$) groups in position 2 of iduronate in **3**.

The interaction energy surfaces were calculated by using GRID18[22] and the corresponding cation as the probe. The spacing between the calculated points was 0.33 Å, the dielectric constants used were 20 for the ligand and 80 for the water. The set of charges was taken from PIM parameters.[32] Three enthalpic components were considered: Lennard-Jones potential, hydrogen bond and electrostatic potential. The calculated surfaces were analysed by using SYBYL6.9[33] by representing the volume above the best interaction energy.

The structures used for calculation of the energy surface with the cations were constructed on the basis of previous explicit solvent MD results,[18] PDB structures deposited in the Protein Data Bank and on recent MD run in vacuo. The values of significant torsion angles were taken from the MD by analysis of their distribution along the trajectories. Sulfate groups orientation has been followed as Φ/Ψ angles and been taken into account for the building of the models used in the GRID search.

Acknowledgements

This research was supported by the Ministry of Science and Technology (Grant BQU2002-03734). F.C. and J.A. are grateful for predoctoral fellowships to the European Union (TMR Programme: GLYCOTRAIN) and Fundación Ramón Areces, respectively.

References

1. Lindhal, U. *Glycoconjugate J.* **2001**, *17*, 597–605.
2. Casu, B.; Lindhal, U. *Adv. Carbohydr. Chem. Biochem.* **2001**, *57*, 159–206.
3. Conrad, H. E. *Heparin Binding Proteins*; Academic: San Diego, 1998.
4. Mulloy, B.; Linhardt, R. J. *Curr. Opin. Struct. Biol.* **2001**, *11*, 623–628.
5. Kan, M.; Wang, F.; Xu, F.; Craab, J. W.; Hon, J.; McKeehan, W. L. *Science* **1993**, *259*, 1918–1921.
6. Capila, I.; Hernaiz, M. J.; Mo, Y. D.; Mealy, T. R.; Campos, B.; Dedman, J. R.; Linhardt, R. J. *Structure* **2001**, *9*, 57–64.
7. Manning, G. S. *Acc. Chem. Res.* **1979**, *12*, 443–449.
8. Rabenstein, D. L.; Robert, J. M.; Peng, J. *Carbohydr. Res.* **1995**, *278*, 239–256.
9. Liang, J. N.; Chakrabarti, B.; Ayotte, L.; Perlin, A. S. *Carbohydr. Res.* **1982**, *106*, 101–109.
10. Rej, R. N.; Holme, K. R.; Perlin, A. S. *Can. J. Chem.* **1990**, *68*, 1740–1745.
11. Rej, R. N.; Holme, K. R.; Perlin, A. S. *Carbohydr. Res.* **1990**, *207*, 143–152.
12. Angulo, J.; de Paz, J. L.; Nieto, P. M.; Martin-Lomas, M. *Isr. J. Chem.* **2000**, *40*, 289–299.
13. Chevalier, F.; Angulo, J.; Lucas, R.; Nieto, P. M.; Martin-Lomas, M. *Eur. J. Org. Chem.* **2002**, 2367–2376.
14. De Paz, J. L.; Angulo, J.; Lassaletta, J.-M.; Nieto, P. M.; Redondo-Horcajo, M.; Lozano, R. M.; Giménez-Gallego, G.; Martin-Lomas, M. *ChemBioChem.* **2001**, *2*, 673–685.

15. Lucas, R.; Angulo, J.; Nieto, P. M.; Martin-Lomas, M. *Org. Biomol. Chem.* **2003**, *1*, 2253–2266.
16. Mulloy, B.; Forster, M. J.; Jones, C.; Drake, A. F.; Johnson, E. A.; Davies, D. B. *Carbohydr. Res.* **1994**, *255*, 1–26.
17. Yates, E. A.; Santini, F.; De Cristofano, B.; Payre, N.; Cosentino, C.; Guerrini, M.; Naggi, A.; Torri, G.; Hricovini, M. *Carbohydr. Res.* **2000**, *329*, 239–247.
18. Angulo, J.; Martin-Lomas, M.; Nieto, P. M. in preparation.
19. Mulloy, B.; Foster, M. *Glycobiology* **2000**, *10*, 1147–1156.
20. Ferro, D.; Provasoli, A.; Ragazzi, M.; Casu, B.; Torri, G.; Bossennec, V.; Perly, B.; Sinay, P.; Petitou, M.; Choay, J. *Carbohydr. Res.* **1990**, *195*, 157–167.
21. Goodford, P. S. *J. Med. Chem.* **1985**, *28*, 849–857.
22. Braccini, I.; Grasso, R. P.; Pérez, S. *Carbohydr. Res.* **1999**, *317*, 119–130.
23. Angulo, J.; Nieto, P. M.; Martin-Lomas, M. *Chem. Commun.* **2003**, 1512–1513.
24. Verkhivker, G. M.; Bouzida, D.; Gehlhaar, D. K.; Rejto, P. A.; Freer, S. T.; Rose, P. W. *Curr. Opin. Struct. Biol.* **2002**, *12*, 197–203.
25. Aqvist, J.; Luzhkov, V. B.; Brandsdal, B. O. *Acc. Chem. Res.* **2002**, *35*, 358–365.
26. Davis, A. L.; Lane, E. D.; Keeler, J.; Moskau, D.; Lohman, J. *J. Magn. Reson.* **1991**, *94*, 637–644.
27. Bax, A.; Davis, D. G. *J. Magn. Reson.* **1985**, *65*, 355–360.
28. Jeener, J.; Meier, B. H.; Bachmann, P.; Ernst, R. R. *J. Chem. Phys.* **1983**, *71*, 4546–4553.
29. Marion, D.; Wüthrich, K. *Biochem. Biophys. Res. Commun.* **1983**, *113*, 967–974.
30. Case, D. A.; Pearlman, D. A.; Caldwell, J. W.; Cheatham, T. E., III; Ross, W. S.; Simmerling, C. L.; Darden, T. A.; Merz, K. M; Stanton, R. V.; Cheng, A. L.; Vincent, J. J.; Crowley, M.; Tsui, V.; Radmer, R. J.; Duan, Y.; Pitera, J.; Massova, I.; Seibel, G.; Singh, U. C.; Weiner, P. K.; Kollman P. A. AMBER6, University of California San Francisco, San Francisco, CA, 1996.
31. Woods, R. J.; Dwek, R. A.; Edge, C. J.; Fraiser-Reid, B. *J. Phys. Chem.* **1995**, *99*, 3832–3846.
32. Pérez, S.; Meyer, C.; Imberty, A. Structure of acetylcholinesterase and its complexes with anticholinesterase agents. In *Modelling of Biomolecular Structures and Mechanisms*; Pullman, A., Jortner, J., Pullman, B., Eds.; Kluwer Academic: Dordrecht, 1995; pp 425–444.
33. SYBYL®6.8, Tripos Inc., 1699 South Harley Rd., St. Louis, Missouri 61344, USA.